Available online at www.sciencedirect.com
SCIENCE DIRECT®

Cold Regions Science and Technology 37 (2003) 227–232

cold regions science and technology

www.elsevier.com/locate/coldregions

Structural phase changes of the liquid water component in Alpine snow

A. Denoth*

Institute of Experimental Physics, University of Innsbruck, Technikerstrasse 25/4, A-6020 Innsbruck, Austria

Received 1 September 2002; received in revised form 29 April 2003; accepted 2 July 2003

Abstract

The arrangement of free water in the complex texture of Alpine snow was measured by different methods: broadband electro-magnetic measurements ranging from radio frequencies up to the microwave K-Band regime directly allow the detection of the geometrical structure of the water bodies; hydraulic measurements—measurements of water percolation through or water drainage off an Alpine snow cover—show a significant change of water movement characteristics which are caused by changes in the water geometrical configuration (structural phase changes) due to the natural variation in the free water saturation. Structural characteristics of water bodies included in snow are reflected by the dielectric depolarization factors. The special case of ring-shaped water inclusions is reflected by the magnetic permeability. Field measurements were carried out in the Stubai Alps, Austria. Metamorphism of these Alpine snow covers was characterized by several melt–freeze cycles. Four main regimes of water saturation existed, each characterized by different structural properties of the free water bodies: the pendular zone with closed isolated water bodies, a funicular zone with confluent water bodies, a transitional zone where isolated water bodies begin to merge and a sub-regime included in the pendular zone characterized by the existence of ring-shaped water bodies. Experimental results of a 12-year field study are presented.

Keywords: Snow physics; Electromagnetic properties; Hydraulic properties; Snow liquid water content; Wet snow

---

1. Introduction

Liquid water in snow generally exists in different geometric arrangements depending on the amount of water present: the pendular regime with two different sub-zones, the funicular regime, a pendular–funicular transition zone and the regime of complete saturation (Colbeck, 1982; Denoth, 1999). The pendular regime is characterized by isolated closed water bodies and ranges from the adsorbed-liquid limit to saturations at which some of the water bodies coalesce. Recently, the existence of closed ring-shaped water bodies within the pendular regime of Alpine snow which has experienced several freeze–thaw cycles has been proved by electromagnetic measurements (Denoth, 1999) and by analyzing shock-frozen samples of wet snow (Brzoska et al., 1998). The funicular regime at higher saturations shows continuous liquid paths throughout the pore space with an isolated and trapped gaseous phase. The actual arrangement and geometry of the individual components of wet snow—ice, water

---

* Fax: +43-512-507-2921.
E-mail address: armin.denoth@uibk.ac.at (A. Denoth).

0165-232X/$ - see front matter © 2003 Elsevier B.V. All rights reserved.
doi:10.1016/S0165-232X(03)00066-1

and air—influence both the electromagnetic and hydraulic response, and this offers a way to experimentally determine water geometry in the different saturation regimes. Experimental results of a 12-year field study are given. Field measurements have been carried out in the Stubai Alps in Austria. Old or firn-type snow was used with mean grain sizes exceeding 1 mm in diameter and which had experienced several melt–freeze cycles.

2. Methods and materials

Electromagnetic and hydraulic measurements were done with old or firn-type wet Alpine snow with mean grain sizes exceeding 1 mm. Grain shape and size were derived from photographical analysis of the individual snow samples (Denoth, 1982). Snow liquid water content W was measured with a calibrated dielectric probe (Denoth, 1994). Snow porosity Φ was calculated from measured density. Snow water saturation S was derived according to $S = W/\Phi$.

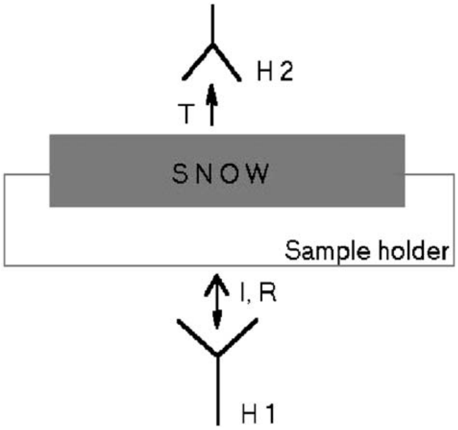

Fig. 1. Free-space technique. H1, H2: horn antennas, I, R, T: incident, reflected and transmitted signal.

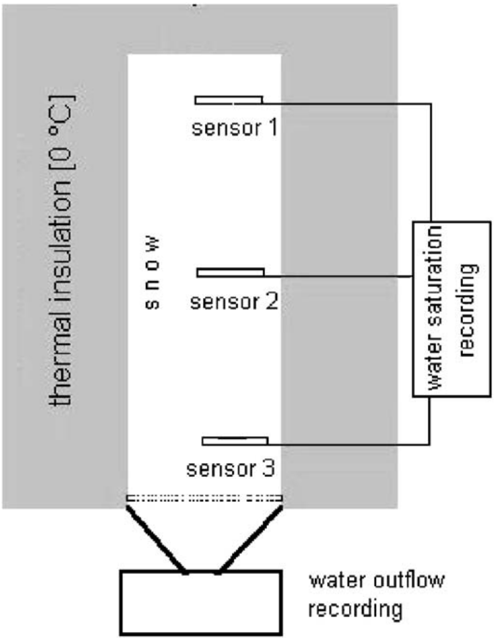

Fig. 2. Block diagram of the experimental setup for drainage measurements. The variation of the local water content with time was recorded at three different levels by dielectric probes.

Electromagnetic measurements were done using a free-space technique, with the snow sample placed in between two high-gain microwave horn antennas. The principle of operation is shown in Fig. 1. Reflected and transmitted signals were measured in the frequency range of 6–16 GHz by a network analyzer, model HP8510A (Denoth, 1999). Based on Fresnel's formulae, snow dielectric permittivity $\varepsilon = \varepsilon' - \mathrm{i}.\varepsilon''$ and magnetic permeability $\mu = \mu' - \mathrm{i}.\mu''$ were derived from the measured total reflection and transmission coefficients. Data analysis to derive structural parameters of the liquid water component is based on the effective-medium model of Polder and van Santen (1946):

$$\varepsilon = (1/3)\{3 + (\varepsilon_{\mathrm{i}} - 1)(1 - \Phi)\Sigma_k[\varepsilon/(\varepsilon + (\varepsilon_{\mathrm{i}} - \varepsilon)G_{k\mathrm{i}})] + (\varepsilon_{\mathrm{w}} - 1)W\Sigma_k[\varepsilon/(\varepsilon + (\varepsilon_{\mathrm{w}} - \varepsilon)G_{k\mathrm{w}})]\}$$

with ε, ε_{i}, ε_{w} are the dielectric permittivity of the mixture, ice and water, respectively. In this model, the geometry of the solid (ice) and the liquid (water) components is described by three-axial ellipsoidal bodies, and is characterized by the corresponding depolarization factors in the direction of the principal axes for the ice component $G_{k\mathrm{i}}$ and the water component $G_{k\mathrm{w}}$ with $k = 1, 2, 3$ and $\Sigma_k G_k = 1$ (Sihvola, 1999). Measured snow magnetic permeability is interpreted in terms of the induced diamagnetic effect of conducting water rings around contact zones of ice grains, whereby the fraction of total water forming the rings has been used as a fitting parameter (Denoth, 1999). So, the geometrical shape of the water inclusions and the

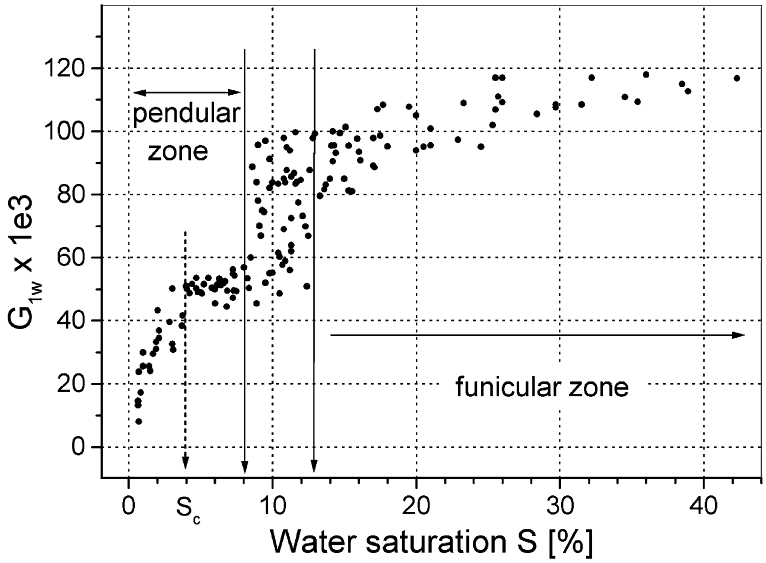

Fig. 3. Dependence of shape factor G_{1w} on liquid water saturation S. Regions with significant changes in the shape factor are marked by arrows.

amount of water collected in the special shape of pendular rings can be derived from electromagnetic measurements. It is obvious that changes in water geometry and arrangement affect the flow characteristics of water in snow. Consequently, additional information e.g. on the amount of bound or immobile water within the pendular zone can be obtained. In addition to the electromagnetic measurements, water movement through snow was studied in the field by long-term drainage experiments. Drainage characteristics were studied by using cylindrical aluminium tubes of 0.25 m in diameter and lengths of 1.38 and 1.98 m filled with sieved natural snow. Initial liquid water saturation, snow porosity and mean grain size

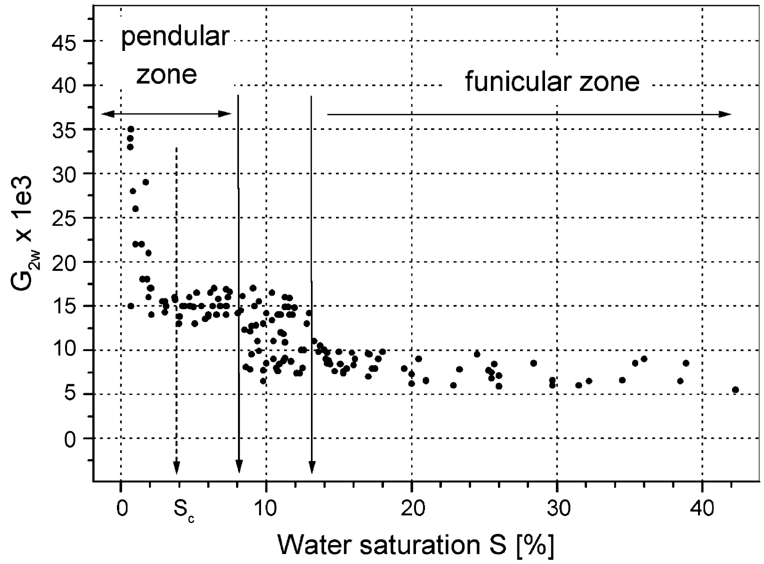

Fig. 4. Dependence of shape factor G_{2w} on liquid water saturation S. Regions with significant changes in the shape factor are marked by arrows.

were measured. The tubes were set upright in deep snow and have been covered with a snow layer of at least 0.75 m thickness to guarantee isothermal conditions during the experiment (Denoth et al., 1979; Wilhelm et al., 1992). At a 1-h time interval, local snow liquid water content was measured automatically at three different heights within the snow column using calibrated dielectric probes. The sensors were placed vertically in the snow column to minimize their influence on water drainage. A sketch of the experimental set-up is given in Fig. 2.

3. Experimental results

Dielectric (ε', ε'') and magnetic (μ', μ'') permeabilities of a total of 151 snow samples were measured in the frequency range of 6–16 GHz. Water saturation S of the natural snow samples varied from 0% to 40%. Based on the effective medium model of Polder and van Santen (1946), the characteristic shape factors of the water inclusions $G_{k\mathrm{w}}$ were derived using least-square fitting routines. The permeabilities ε' and ε'' of the solid and liquid water components have been calculated according to a Debye-like model (Ulaby et al., 1986). The characteristic shape factors of the solid ice inclusions $G_{k\mathrm{i}}$ were derived from a photographical analysis of the individual snow samples (Denoth, 1982). Considering the relative high-measurement frequencies, the effect of ionic conductivity to the total dielectric losses has been neglected. Figs. 3 and 4 show the dependence on water saturation of the shape factors $G_{1\mathrm{w}}$ and $G_{2\mathrm{w}}$, respectively; $G_{3\mathrm{w}}$ can easily be derived from $G_{3\mathrm{w}} = 1 - G_{1\mathrm{w}} - G_{2\mathrm{w}}$. Regions where significant changes in the shape factors can be observed are marked by arrows. Both shape factors $G_{1\mathrm{w}}$ and $G_{2\mathrm{w}}$ varied significantly with water saturation: funicular and pendular saturation regimes are clearly separated by a transitional zone ranging from about 8% to 13% of the pore volume. Within the pendular regime at liquid saturations S lower than a critical saturation $S_c \approx 4\%$, a sub-zone is formed characterized by a strongly decreasing shape factor $G_{1\mathrm{w}}$: $G_{1\mathrm{w}} \rightarrow 0$, and increasing shape factor $G_{2\mathrm{w}}$: $G_{2\mathrm{w}} \rightarrow 0.07$. In the sub-zone $0 < S < S_c$, capillary forces and surface tension may control the geometric shape of the water inclusions. For $S > S_c$, gravity forces may play the dominant role. The dependence of magnetic loss μ'' on water saturation is shown in Fig. 5 for a selected frequency $f = 14$ GHz. Regions where significant changes in the

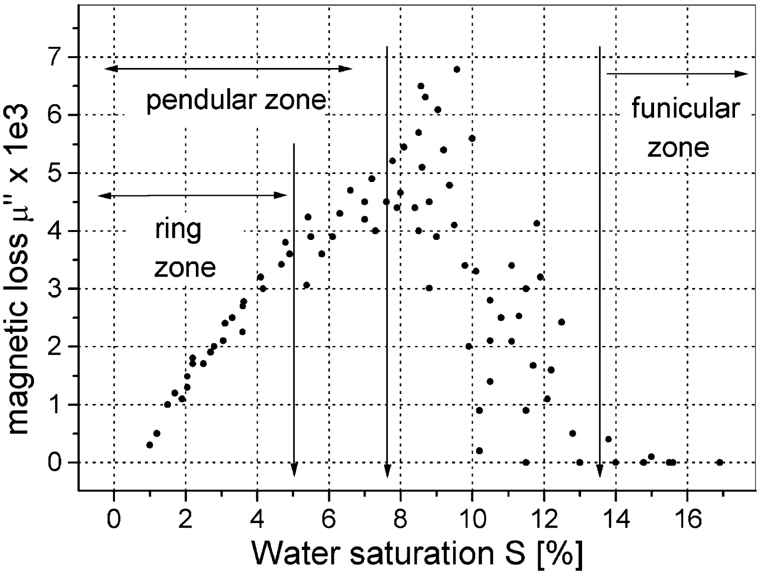

Fig. 5. Dependence of magnetic loss μ'' (at $f = 14$ GHz) on water saturation S. Regions with significant changes in the loss factor are marked by arrows.

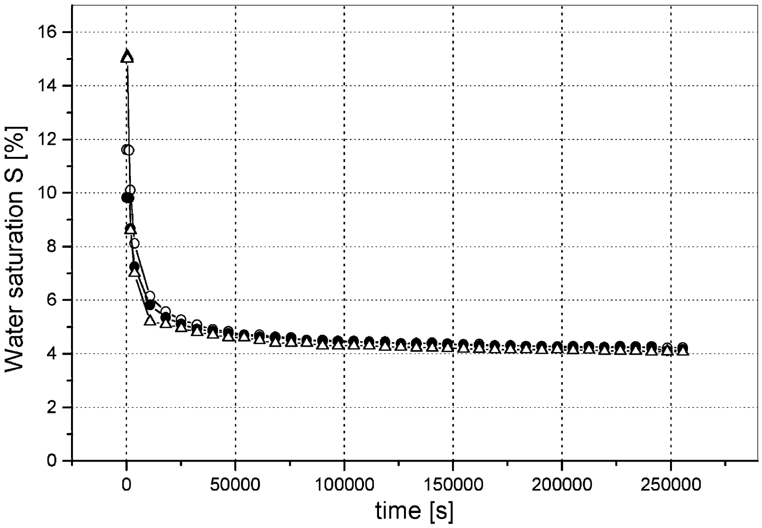

Fig. 6. Long-term variation of water saturation S with time at a depth of 1.6 m below the surface of a draining snow column shown for three different initial conditions: $S(t=0)=11.6\%$ (open circles), $S(t=0)=9.8\%$ (solid circles) and $S(t=0)=15\%$ (open triangles).

'induced' diamagnetic losses can be observed are marked by arrows.

Compared to the intrinsic magnetic permeability of bulk water ($\mu' \cong 1$, $\mu'' \cong 0$), the relative high apparent magnetic losses are caused by electrically conducting ring-shaped water bodies. The range of existence, however, is limited to low water saturations, well within the pendular regime: for saturations less than approximately 5% more or less all the free water seems to be arranged in ring-like structures. For saturations exceeding $S \approx 8\%$, magnetic losses decrease drastically, indicating a merging of water rings whereby closed spheroidal water bodies are formed. This transitional zone is followed by a zone characterized by $\mu''=0$, and this zone compares favorably with the funicular zone defined by the shape factors G_{kw}.

Typical long-term variations of water saturation $S(t)$ with time at a depth of 1.6 m below the surface of a draining snow column are shown in Fig. 6 for three different initial snow conditions:

(a) $S(t=0)=11.6\%$, $\Phi=0.49$, mean grain size: 1.4 mm, marked by open circles,
(b) $S(t=0)=9.8\%$, $\Phi=0.44$, mean grain size: 2 mm, marked by solid circles, and
(c) $S(t=0)=15\%$, $\Phi=0.51$, mean grain size: 1.5 mm, marked by open triangles.

Independent of the initial conditions, water saturation S approaches asymptotically a limiting value $S_i \approx 4\%$ denoted as irreducible saturation with $S_i = S(t \rightarrow \infty)$.

It may be of interest that S_i, the irreducible water saturation, excellently compares to the critical saturation S_c derived by electromagnetic measurements, and S_c and S_i may be identical. Consequently, the saturation zone $0<S\leq S_c \equiv S_i$ within the pendular regime is characterized by the dominance of capillary/surface forces over gravitational forces.

4. Conclusion

Measurement data presented on the electromagnetic response of wet coarse-grained Alpine snow which had experienced freeze–thaw cycles together with experimental results from thin sections of shock-frozen wet snow reported by Brzoska et al. (1998) confirm the existence of ring-shaped water bodies for saturations less than a critical saturation $S_c \approx 4\%$. In addition, S_c compares well to the irreducible saturation S_i derived from drainage experiments. The saturation zone $0<S\leq S_c \equiv S_i$ within the pendular regime is considered as a saturation zone where surface forces dominate over gravity forces. This regime is part of the pendular regime that extends to a saturation of

$S \approx 8\%$ characterized by the increasing importance of gravity forces. The transition from the pendular regime to the funicular regime occurs in a relatively broad range of saturations between $S \approx 8\%$ and $S \approx 14\%$, and is characterized by merging water bodies building up continuous liquid paths.

Acknowledgements

The ‘Wintersport Tirol’ is thanked for supporting in part the field experiments made in the Stubai glacier area.

References

Brzoska, J.-B., Coleou, C., Lesaffre, B., 1998. Thin-sectioning of wet snow after flash-freezing. J. Glaciol. 44 (146), 54–62.

Colbeck, S.C., 1982. The geometry and permittivity of snow at high frequencies. J. Appl. Phys. 53 (6), 4495–4500.

Denoth, A., 1982. Effect of grain geometry on electrical properties of snow at frequencies up to 100 MHz. J. Appl. Phys. 53 (11), 7496–7501.

Denoth, A., 1994. An electronic device for long-term snow wetness recording. Ann. Glaciol. 19, 104–106.

Denoth, A., 1999. Wet snow pendular regime: the amount of water in ring-shaped configurations. Cold Reg. Sci. Technol. 30, 13–18.

Denoth, A., Seidenbusch, W., Blumthaler, M., Kirchlechner, P., Ambach, W., Colbeck, S.C., 1979. CRREL Res. Rep. 79-1, Hanover, NH.

Polder, D., van Santen, J.H., 1946. The effective permeability of mixtures of solids. Physica 12 (5), 257–271.

Sihvola, A., 1999. Electromagnetic mixing formulas and applications. IEE Electromagn. Waves Ser. 47 (IEE, London, UK).

Ulaby, F.T., Moore, R.K., Fung, A.K., 1986. Microwave Remote Sensing Active and Passive, vol. III: From Theory to Applications Artech House, Dedham, MA 02026, ISBN 0-89006-192-0.

Wilhelm, T., Rechenmacher, J., Denoth, A., 1992. Transport of water and dye tracers through snow. Proc. Int. Snow Science Workshop, Breckenridge, CO, USA, October 4–8, 1992, 365–370.